OPEN

Counterflow Dielectrophoresis for Trypanosome Enrichment and Detection in Blood

Anoop Menachery[1]*, Clemens Kremer[1]*, Pui E. Wong[2], Allan Carlsson[1], Steven L. Neale[1], Michael P. Barrett[2] & Jonathan M. Cooper[1]

[1]Department of Electronics and Electrical Engineering, The Bioelectronics Research Centre, College of Science and Engineering, Rankine Building, University of Glasgow, Glasgow, G12 8LT, Scotland, U.K., [2]Wellcome Trust Centre for Molecular Parasitology, Institute of Infection, Immunity and Inflammation, College of Medical, Veterinary and Life Sciences Sir Graeme Davies Building, 120 University Place, G12 8TA, Scotland, U.K.

Human African trypanosomiasis or sleeping sickness is a deadly disease endemic in *sub-Saharan* Africa, caused by single-celled protozoan parasites. Although it has been targeted for elimination by 2020, this will only be realized if diagnosis can be improved to enable identification and treatment of afflicted patients. Existing techniques of detection are restricted by their limited field-applicability, sensitivity and capacity for automation. Microfluidic-based technologies offer the potential for highly sensitive automated devices that could achieve detection at the lowest levels of parasitemia and consequently help in the elimination programme. In this work we implement an electrokinetic technique for the separation of trypanosomes from both mouse and human blood. This technique utilises differences in polarisability between the blood cells and trypanosomes to achieve separation through opposed bi-directional movement (cell counterflow). We combine this enrichment technique with an automated image analysis detection algorithm, negating the need for a human operator.

Human African trypanosomiasis (HAT) is a deadly parasitic disease endemic in *sub-Saharan* Africa. The parasites are transmitted by tsetse flies and live in the human bloodstream, before invading the tissues of the central nervous system, where they cause severe neurological disorders. The recent decline in incidence of HAT has led to an optimism that the disease might be eliminated[1] and the World Health Orgnaisation has set 2020 as a date to achieve this[2]. However, the chronic nature of the disease (with infections often lasting in advance of four years), low parasitaemia and lack of specific symptoms associated with early stages of the disease, will confound this process unless improved diagnostic tools become available.

The parasite is most commonly detected by examination of a smear of blood or lymph node aspirate, providing a straightforward, low sensitivity detection method of verifying infection in the individual[3–5]. The sensitivity of such direct detection methods can be improved by combining visual observation with enrichment techniques such as whole blood centrifugation[6] and mini-anion exchange chromatography, followed by centrifugation[7]. PCR based amplification has also proved its effectiveness in the detection of trypanosome DNA in whole blood, lymph node fluid or cerebrospinal fluid. Complex experimental requirements have hindered the implementation of PCR-based diagnostics in the field, but isothermal DNA amplification techniques are currently showing promise[8]. Notwithstanding these advances there is currently a need for the development of new methods that can be readily implemented in a resource poor environment, without the need for an expert operator.

Miniaturization of trypanosome diagnostic tests have the potential to improve the ability to process and analyse samples. Lab-on-chip platforms can readily combine electrical, optical and fluidic technologies to enable point-of-care diagnostics. For example, a recent application of deterministic lateral displacement in a microfluidic device has shown the separation of the model organism, *Trypanosoma cyclops,* from red blood cells (RBCs)[9].

In this paper, we now show how dielectrophoresis (DEP), defined as the movement of cells as a result of the interaction of the induced dipole moment with a spatially non-uniform electric field[10,11], can be used to enrich trypanosomes within blood. In conventional DEP configurations, electrode arrays are connected to an AC voltage to generate stationary non-uniform electric fields. This induces a short translational motion of cells, either to or from regions of high electric field intensity, based on their effective polarisabilities. The movement of cells

towards regions of high electric field magnitude, typically electrode edges, is defined as positive DEP, whereas movement away from these regions is defined as negative DEP.

As an alternative, in order to induce translational motion of cells over larger distances, without the use of external pumps or fluid actuators, adjacent electrodes were energised with AC signals which are phase shifted by 90°. In this case, a cell is subjected to a travelling field, a mechanism which is referred to as travelling wave dielectrophoresis (TWDEP)[10].

DEP has been used to enrich various mammalian cell types including breast carcinoma cells[12], putative stem cells from adipose tissue[13] and multi-drug resistant leukemic cells[14]. Gascoyne et al. have also successfully demonstrated the use of DEP for the separation of *Plasmodium* infected blood cells from normal RBCs[15].

We now demonstrate a new technique enabling differential movement of cells based not only upon their biophysical properties, but also the fact that the microorganism (but not the RBC) is motile (i.e. the intrinsic ability of a cell or microorganism for self propulsion). The particular electrode geometry, coupled with the phase difference in the fields results in the motile cells being moved into particular regions of field gradient, resulting in simultaneous opposing motion of trypanosomes and RBCs.

The spatially dependent phase and magnitude of the electric field can be described by

$$E = E_{xo}\cos(\omega t + \varphi_x)\hat{i} + E_{yo}\cos\left(\omega t + \varphi_y\right)\hat{j} + E_{zo}\cos(\omega t + \varphi_z)\hat{k} \quad (1)$$

where ω is the angular frequency of the field, (E_{xo}, E_{yo}, E_{zo}) and $(\varphi_x, \varphi_y, \varphi_z)$ are the spatially dependent components of the field magnitude and phases respectively. The DEP force comprises the sum of two components, $F_{DEP} = F_{cDEP} + F_{TWDEP}$, the first being a result of the interaction of the in-phase component of the dipole moment with the field magnitude non-uniformity (F_{cDEP}) whilst the second (F_{TWDEP}) is a result of the interaction of the out-of-phase dipole moment with the field phase non-uniformity[16–18]. The dipole approximation of the DEP force can be written as;

$$F_{DEP} = 2\pi V \varepsilon_m$$
$$\left(0.5 RE(CM)\nabla E^2 + IM(CM)\left(E_{xo}^2\nabla\varphi_x + E_{yo}^2\nabla\varphi_y + E_{zo}^2\nabla\varphi_z\right)\right) \quad (2)$$

where the first and second terms correspond to F_{cDEP} and F_{TWDEP} respectively, V is the volume of the cell, ε_m is the permittivity of the suspending medium and the Clausius Mosotti (CM) factor is a complex term which depends on the polarisability of the cell with respect to the surrounding medium. It describes the Maxwell-Wagner relaxation that occurs at the interfaces between dissimilar dielectrics such as the particle and medium. The magnitude and direction of the DEP force is given by the CM factor and the electric field non-uniformities.

In general, the mechanism for selective cell enrichment is dependent on the biophysical differences (mostly size and shape) between cell types. The DEP force acts on cells (which have no net charge) regardless of surface charge, unlike existing methods used to enrich trypanosomes (mini-anion exchange chromatography). The DEP response is typically characterized by a cross-over frequency, where a viable cell experiences a transition from negative DEP (i.e a force away from area of high electric field) to positive DEP (i.e a force towards areas of high electric field), and thus experiences no force at this frequency. The cross-over frequency is an experimentally measured parameter, commonly used as a determinant for cell characterization and separation (see supporting information). Our results describe the use of such a travelling electric field to manipulate trypanosomes and RBCs to different spatial field regions, thereby achieving enrichment of trypanosomes from blood. This offers the potential to transform trypanosome diagnosis.

Results

Modelling. First, we modelled how motile trypanosomes move relative to red blood cells in TWDEP. To understand the influence of the travelling electric field, simulations were performed using *COMSOL Multiphysics* with a 2D geometric model of adjacent electrodes with a 30 μm spacing (Fig. 1). For TWDEP, four signals with phase shifts of 90° were used to generate a travelling electric field with a spatially dependent phase. The values for the real and imaginary part of the electric potential were assigned a peak amplitude of 1V, corresponding to the experimental conditions. After imposing the necessary boundary conditions[19], the potential distribution was determined. The electric field E is calculated using $E = -\nabla V$, and this is used to estimate the DEP force components. For the full details on the model used, please refer to the supplementary information.

In Fig. 2 (a), the ∇E^2 vector direction for positive DEP conditions ($Re(CM) > 0$) is vertically downwards onto the electrode edges while for negative DEP conditions ($Re(CM) < 0$), the vector arrows will be directed upwards (reverse orientation to those shown in Fig. 2 (a)), resulting in the levitation of cells above the electrode plane.

Figure 2 (b) shows the direction and magnitude of the $E_{xo}^2\nabla\varphi_x + E_{yo}^2\nabla\varphi_y + E_{zo}^2\nabla\varphi_z$ vectors above a four-phase electrode array. It can be observed that for heights > 10 μm above the electrode plane, the vectors point to the right, but for heights < 10 μm, these vectors point in the opposite direction.

The vector directions in Fig. 2 (c) demonstrate that for RBCs, a combination of $Re(CM) < 0$ and $Im(CM) > 0$ results in levitation to a height > 20 μm followed by anti-field TWDEP translational motion away from the centre of the device. For trypanosomes, a combination of $Re(CM) > 0$ and $Im(CM) > 0$ results in attraction to the electrode plane followed by translational movement in the opposite direction to the RBCs (Fig. 2 (d)). The change in direction is a result of the reversal of the field phase non-uniformity factor ($E_{xo}^2\nabla\varphi_x + E_{yo}^2\nabla\varphi_y + E_{zo}^2\nabla\varphi_z$) at heights < 10 μm. In effect, the RBCs are pushed upwards and outwards from the centre, whilst the trypanosomes are pulled downwards and inwards. The magnitude of the force is larger at the plane of the electrodes and decreases rapidly with increases in height. The net result is the separation of parasites and RBCs due to their motion in opposite directions.

Trypanosome enrichment using traveling wave dielectrophoresis. Based upon the proposed mechanism and the theoretical model outlined above, we applied a trypanosome-red cell mixture to a spiral electrode array and applied a quadrature-phase voltage of 140 kHz and 2V pk-pk. Under these conditions, a travelling electric field was generated which induces levitation and translational
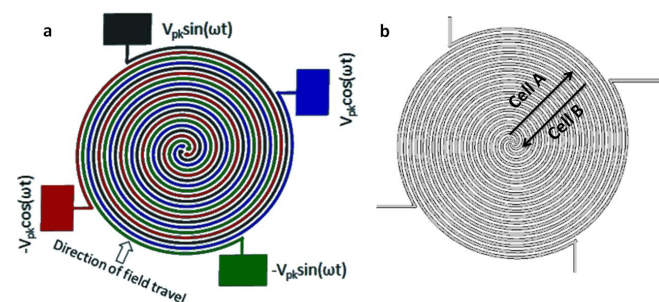

Figure 1 | Electrode array used in this work. (a) Schematic of the four arm spiral microelectrode array comprising four parallel spiral elements of 30 μm in width and spacing. The electrodes are energized with a 90° phase shift respective to each other. (b) Working principle of the chip. While cell type A (e.g. red blood cells) is expelled from the electrode array, cell type B (e.g. trypanosomes) is concentrated into the centre of the array. Both processes take place simultaneously.
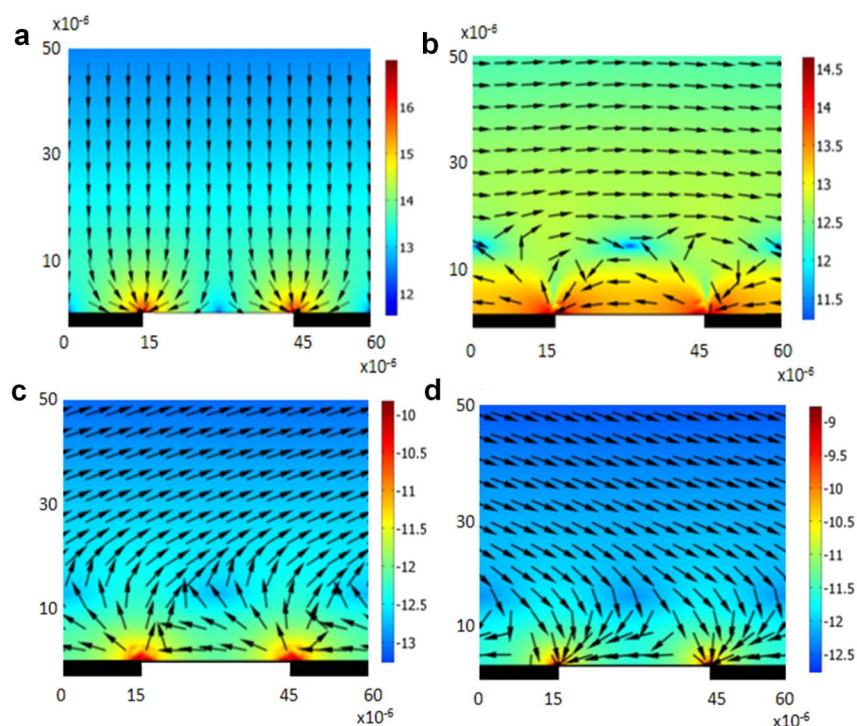
Figure 2 | A vertical section along the electrode plane showing the spatial variation of the DEP force components. The arrows represent the vector direction of the force components and the surface plot represents the magnitude of the force components (V^2/m^3, log$_{10}$ scale). The x and y scale are in metres. (a) Shows a spatial variation of ∇E^2 whilst (b) shows a spatial variation of $E_{xo}^2\nabla\varphi_x + E_{yo}^2\nabla\varphi_y + E_{zo}^2\nabla\varphi_z$ (both are for the same cell type). (c) and (d) show the combined forces of ∇E^2 and $E^2\nabla\varphi$ for mouse RBCs (c) and trypanosomes (d) both at 140 kHz.

anti-field motion of the RBCs towards the outer edges of the spiral (Fig. 3 (a–d)). Under the same conditions the trypanosomes were attracted to the electrode plane and underwent translational movement into the centre of the spiral electrode array (Fig. 3 (c–e)), in accordance with the predictions of modeling outlined above.

Upon entering the centre of the spiral, the trypanosomes underwent translational movement in a circular orbit (Fig. 3 (e)). After a period of 10 minutes of trypanosome enrichment, an AC voltage shift from a quadrature-phase to an opposing two-phase field caused the translational and rotational movement to cease, resulting in the capture of the trypanosomes between the electrode edges due to positive DEP (Fig. 3 (f)).

At the end of the enrichment process, white blood cells were never observed in the centre of the spiral, their size ensuring a positive DEP response trapping them at the electrode edges, while platelets and any small-to-medium sized cells experienced negative DEP and were cleared to the outer edges of the spiral along with the RBCs.

The velocity and enrichment numbers of trypanosomes, in the travelling wave experiments, were measured as a function of the applied voltage for a fixed frequency of 140 kHz, and results are shown in Supplementary Fig. S7 online. Enrichment number denotes the number of trypanosomes collected in the centre of the spiral array during the course of an experiment (normalised in order to account for varying parasite concentrations). The applied voltage was increased from 2 to 4V pk-pk and consequentially the velocity was found to increase from 3 μm/sec to 11 μm/sec. It was observed that at voltages higher than 2V pk-pk the trypanosomes underwent lysis when entering the central region.

The velocity and enrichment numbers were also measured as a function of the applied AC frequency for a fixed voltage of 2V pk-pk, and a value of 140 kHz was found to be optimal for the concentration of trypanosomes from RBCs, results shown in Supplementary Fig. S7 online. Enrichment of Trypanosomes from human blood was demonstrated at 100 kHz and 2 Vpk-pk respectively.

The process of clearing the RBCs to the outer edge of the spiral takes approximately 5 minutes, whereas the final enrichment of trypanosomes at the spiral's centre takes ~5 minutes longer due to periods of entrapment at the electrode edges (for quadrature-phase voltage signals of 2V pk-pk and 140 kHz, trypanosomes are trapped for an average of ~6.5 seconds at the electrode edges compared to ~2 seconds to travel between adjacent electrodes). The total time for the process of enrichment was 10 minutes.

Automated detection algorithm. In order to further demonstrate how this bidirectional TWDEP setup could enable a point of care device in trypanosome diagnostics we combined it with an automated detection algorithm. An intensity map for each video frame was obtained by the convolution of a steerable filter tuned to match the width of the trypanosomes with a captured frame. Pixel intensity was associated and maximized to facilitate identification of elongated regions of high intensity, (Fig. 4 (a)) and the detected trypanosomes highlighted in green, (Fig. 4 (b)).

Discussion

Here, we demonstrate the bidirectional movement of cells in a traveling wave dielectrophoresis setup that permits enrichment and easy identification of blood parasites. A potential practical application of trypanosome separation is in diagnosis of the diseases caused by these parasites which is currently hindered by low parasitaemias which mean that concentrations steps are needed to enrich parasites prior to microscopic visualisation.

The bidirectional counterflow dielectrophoresis that we describe can be attributed to the fact that immotile small red cells experience a negative dielectrophretic force which repels them from the spiral array of electrodes while larger cells, including pathogenic trypanosomes experience a positive force bringing them to the electrodes. However, as trypanosomes can produce significant forces through their flagellum[20], they are able to propel themselves free of the electrode and
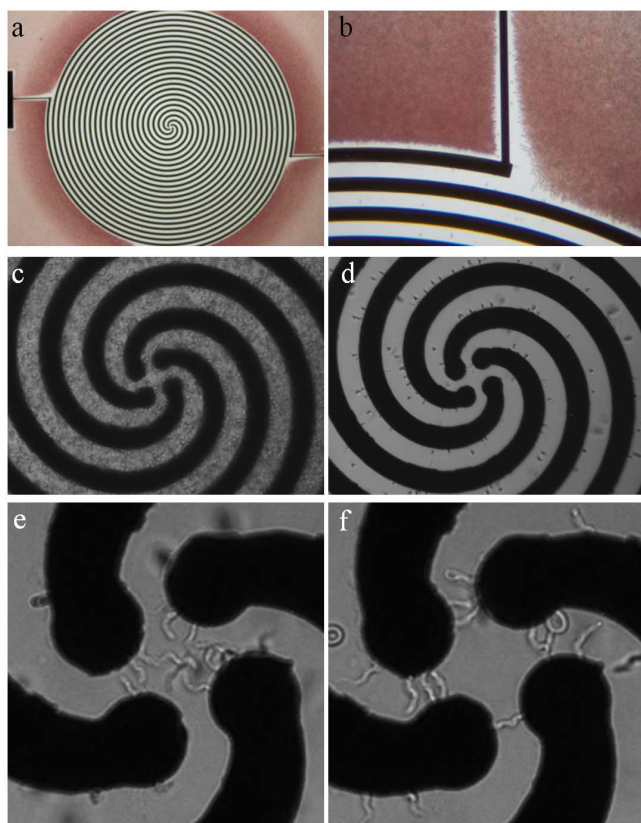
Figure 3 | **Enrichment of trypanosomes from infected blood.** Total width of the spiral array is 2.9 mm, electrode width and spacing is 30 μm. (a,b) Micrograph following a separation process, with the RBCs having been pushed away from the electrode array. (c) Parasitized blood on the spiral electrode array. (d) Mouse RBCs are levitated and carried to the outer edges of the spiral. (e) Trypanosomes accumulate in the centre of the spiral and undergo circular translational motion. (f) Trypanosomes are trapped along the electrode edges in the centre of the spiral upon switching the AC voltage from quadrature-phase to an opposing two-phase.

then experience positive attraction to the next electrode in the spiral. Non –motile cells remain fixed at the electrode to which they are first attracted hence, in time, a pure sample of trypanosomes is concentrated in the middle of the spiral.

At low frequencies, as a result of the capacitive behavior associated with the cell's membrane, the effective polarisability of both cell types is less than that of the surrounding medium. Above the critical cross-over frequency, the effective polarisability of the cell exceeds that of the medium, and the Clausius Mosotti (CM) factor becomes positive. Importantly, the measured cross-over frequency was found to be lower for trypanosomes than RBCs, as shown in Supplementary Fig. S2 online. For viable trypanosomes and for RBCs with intact insulating membranes, the main contributions to the difference in frequency at which each cell type transitions from a negative to positive CM arise due to differences in cell size and shape.

The translational velocity of trypanosomes does not exhibit a dependence on voltage-squared as in the case of conventional DEP. This can be attributed to an increase in both the vertical (z) and horizontal (x,y) components of the force. Additionally, an increase in the applied voltage results in an increase in the downward DEP trapping force, which is evidenced by increased enrichment numbers, shown in Supplementary Fig. S7 online. For optimal enrichment, the maximum voltage was limited to 2V pk-pk to avoid electroporation and lysis of the trypanosomes at the centre of the spiral electrode array.
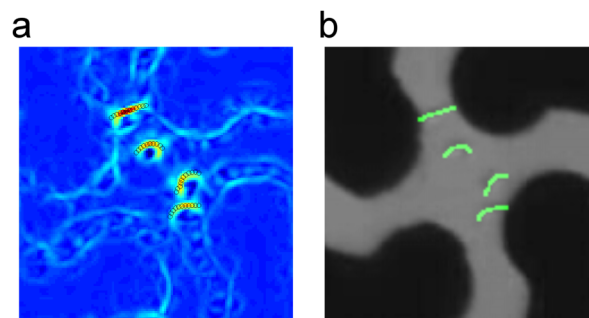

Figure 4 | **Automated detection of trypanosomes in the TWDEP device.** (a) Intensity map using a steerable filter algorithm that emphasises ridges, which appear in yellow/red on the blue background. Trypanosomes are detected by finding fibre like regions of high intensity. (b) The detected trypanosomes are highlighted in green.

The limit of detection of the technique was determined by counting the number of parasites that were concentrated in the centre of the spiral electrode array and comparing it to the expected number of parasites in the sampling volume based on parasite concentration. Operation of a single spiral electrode can detect a minimum parasitemia level of 1.2×10^5 trypanosomes/ml in whole blood. This limit of detection can be improved significantly by increasing the sampling volume, for example a configuration with ten spiral arrays of 1cm diameter each has a predicted detection limit which is two orders of magnitude better, 1.0×10^3 trypanosomes/ml in whole blood (please see supporting information online for details). When comparing the technique with existing methods it should also be noted that sample preparation is fast and simple (dilution takes 5 min) and concentration is also comparatively fast (approximately 10 min). The whole system was designed with a handheld device in mind and the voltage needed to power the electrodes can easily be provided by batteries, providing the ability to perform many assays from a mobile phone, if required.

The addition of an automated detection device for trypanosomes brings novel functionality to any diagnostic test, potentially eliminating the need for a human operator to verify the presence of the parasites. This could enable field clinics to run parallel diagnostic tests utilizing low-cost compact imaging systems in conjunction with this electrokinetic platform. The main advantage of applying a steerable filter, in comparison to a conventional oriented filter, is that the number of required convolutions is reduced significantly and hence the reduced computational intensity allows for real time detection.

The same approach could be applied to any motile parasite including *Trypanosma cruzi* which causes Chagas disease afflicting millions in Latin America, leishmaniasis which infects several million people worldwide as well as macroparasites such as microfilarial worms responsible for diseases like river blindness and elephantiasis. Other motile cells which might be targets for bidirectional TWDEP include bacteria and spermatozoa.

Methods

We characterized the behavior of trypanosomes in mouse blood as a model system. Subsequently we also tested the efficacy of our diagnostic system by demonstrating trypanosome enrichment in human blood (using *in-vitro* grown trypanosomes).

Female adult ICR mice were inoculated with *T. brucei* (strain s427) (1 bloodstraw, ~20 μl of 1×10^8 cells/ml) using intraperitoneal injection. Parasitaemia was monitored daily via tail venepuncture and microscopic observation of blood smears. Mice were culled via a schedule 1 protocol at the desired parasitaemia level (~1×10^8 cells/ml or ~1×10^5 cells/ml). The work involving mice was regulated under the UK home office under project license ppl60/3760 "biochemistry, genetics and immunology of parasitic protozoa" by trained staff holding personal licenses enabling animal handling under the UK animals (scientific procedures) act 1986. Work schedules have been approved by the university of Glasgow ethical review board and the UK home office. Whole blood was collected in CBSS/heparin via cardiac puncture for experimental purposes. Screened human blood was also acquired from the blood

transfusion service. Blood samples were stored at 4°C with anticoagulant and used within 2 days of acquisition.

A DEP supporting medium was prepared containing 3 mM HEPES, pH 7.4 containing 9% sucrose and 0.3% glucose, with an osmolality of 290 mOsm/kg. Prior to enrichment, the cross-over frequencies of trypanosomes and RBCs were characterized in medium conductivities adjusted to specific values between 16 and 60 mS/m by the addition of a phosphate buffered saline solution. The DEP and TWDEP characterization was performed with mouse and human blood that was treated with 0.25% trypsin for 5 minutes to prevent red cell trypanosome agglutination, prior to being washed three times and re-suspended in a specific conductivity medium.

The enrichment was carried out following a two step dilution process circumventing the need for a centrifuge based wash procedure. The sample of blood was first diluted 20 fold and incubated for 5 minutes in the DEP supporting medium containing salt-free trypsin at a concentration of 0.25%, followed by a further 2 fold dilution in the DEP supporting medium containing salt-free trypsin inhibitor at a concentration of 0.25%, resulting in a 40 fold total dilution and a medium conductivity between 40 and 50 mS/m.

Quadrupole electrodes, shown in Supplementary Fig. S3 online, used for characterisation were fabricated using standard photolithographic techniques[21], and consisted of four 200 nm thick gold electrodes vacuum evaporated onto a 10 nm thick seed layer of chromium on glass substrates with polynomial tips arranged at 90° to each other with an interelectrode separation of 400 μm. The crossover frequency for both cell types was determined by observing their movement for electric field frequencies ranging from 10 kHz to 400 kHz and solution conductivity varying from 16 to 60 mS/m.

A 4-arm spiral electrode array[15,22,23] used for our TWDEP experiments, is shown in Fig. 1. The spiral array comprises of four equally spaced electrodes with a width and an inter-electrode separation of 30 μm. The total width of the spiral electrode array was approximately 2.9 mm across and the sample was contained in a square chamber of approximately 6 mm length and a height of 150 μm. A 5 μl sample of diluted blood was pipetted into the chamber (filling it completely) for the purpose of enrichment, but the electrode dimensions limit the effective volume exposed to the electrode array to ~1 μl. The experiments were monitored using an inverted bright field Nikon microscope with a video camera.

After enrichment, the detection of trypanosomes was automated using an image analysis algorithm written in MATLAB (MathWorks), thereby eliminating the need for verification by a human operator. The feature detection algorithm consists of a convolution of each video frame with a steerable ridge detection filter[24,25]. This method has been previously used to determine the position and orientation of individual fibres in flowing suspensions[26]. In this study, the steerable filter was initially adjusted to detect the central region of the spiral electrodes and subsequently highlight the presence of trypanosomes in that region.

1. Welburn, S. C., Maudlin, I. & Simarro, P. P. Controlling sleeping sickness - a review. *Parasitology* **136**, 1943–1949 (2009).
2. WHO. http://www.afro.who.int/en/clusters-a-programmes/dpc/neglected-tropical-diseases/programme-components/human-african-trypanosomiasis-control.html. Accessed 2.1.2012.
3. Chappuis, F., Loutan, L., Simarro, P., Lejon, V. & Buscher, P. Options for field diagnosis of human african trypanosomiasis. *Clin Microbiol Rev* **18**, 133–146 (2005).
4. Barrett, M. P., Boykin, D. W., Brun, R. & Tidwell, R. R. Human African trypanosomiasis: pharmacological re-engagement with a neglected disease. *Br J Pharmacol* **152**, 1155–1171 (2007).
5. Ralston, K. S., Kabututu, Z. P., Melehani, J. H., Oberholzer, M. & Hill, K. L. The Trypanosoma brucei flagellum: moving parasites in new directions. *Annu Rev Microbiol* **63**, 335–362 (2009).
6. Murray, M., Murray, P. K. & McIntyre, W. I. An improved parasitological technique for the diagnosis of African trypanosomiasis. *Trans R Soc Trop Med Hyg* **71**, 325–326 (1977).
7. Lumsden, W. H., Kimber, C. D. & Strange, M. Trypanosoma brucei: detection of low parasitaemias in mice by a miniature anion-exchanger/centrifugation technique. *Trans R Soc Trop Med Hyg* **71**, 421–424 (1977).
8. Njiru, Z. K. *et al.* African trypanosomiasis: sensitive and rapid detection of the sub-genus Trypanozoon by loop-mediated isothermal amplification (LAMP) of parasite DNA. *Int J Parasitol* **38**, 589–599 (2008).
9. Holm, S. H., Beech, J. P., Barrett, M. P. & Tegenfeldt, J. O. Separation of parasites from human blood using deterministic lateral displacement. *Lab Chip* **11**, 1326–1332 (2011).
10. Pethig, R. Review Article-Dielectrophoresis: Status of the theory, technology, and applications. *Biomicrofluidics* **4** (2010).
11. Pohl, H. A. *Dielectrophoresis : The Behavior of Neutral Matter in Nonuniform Electric Fields* (Cambridge University Press, 1978).
12. Kim, U. *et al.* Selection of mammalian cells based on their cell-cycle phase using dielectrophoresis. *Proc Natl Acad Sci U S A* **104**, 20708–20712 (2007).
13. Vykoukal, J., Vykoukal, D. M., Freyberg, S., Alt, E. U. & Gascoyne, P. R. Enrichment of putative stem cells from adipose tissue using dielectrophoretic field-flow fractionation. *Lab Chip* **8**, 1386–1393 (2008).
14. Labeed, F. H., Coley, H. M., Thomas, H. & Hughes, M. P. Assessment of multidrug resistance reversal using dielectrophoresis and flow cytometry. *Biophys J* **85**, 2028–2034 (2003).
15. Gascoyne, P. *et al.* Microsample preparation by dielectrophoresis: isolation of malaria. *Lab Chip* **2**, 70–75 (2002).
16. Wang, X.-B., Huang, Y., Becker, F. F. & Gascoyne, P. R. C. A unified theory of dielectrophoresis and travelling wave dielectrophoresis. *J. Phys. D: Appl. Phys* **27**, 1571–1574 (1994).
17. Morgan, H. & Green, N. G. *AC Electrokinetics: Colloids and Nanoparticles.* (Research Studies Press, 2003).
18. Jones, T. B. *Electromechanics of Particles* (Cambridge Univ. Press, 1995).
19. Green, N. G., Ramos, A. & Morgan, H. Numerical solution of the dielectrophoretic and travelling wave forces for interdigitated electrode arrays using the finite element method. *Journal of Electrostatics* **56**, 235–254 (2002).
20. Rodriguez, J. A. *et al.* Propulsion of African trypanosomes is driven by bihelical waves with alternating chirality separated by kinks. *Proc Natl Acad Sci U S A* **106**, 19322–19327 (2009).
21. Huang, Y., Holzel, R., Pethig, R. & Wang, X. B. Differences in the AC electrodynamics of viable and non-viable yeast cells determined through combined dielectrophoresis and electrorotation studies. *Phys Med Biol* **37**, 1499–1517 (1992).
22. Wang, X. B., Huang, Y., Wang, X., Becker, F. F. & Gascoyne, P. R. Dielectrophoretic manipulation of cells with spiral electrodes. *Biophys J* **72**, 1887–1899 (1997).
23. Goater, A. D., Burt, J. P. H. & Pethig, R. A combined travelling wave dielectrophoresis and electrorotation device: applied to the concentration and viability determination of Cryptosporidium. *Journal of Physics D: Applied Physics* **30** (1997).
24. Freeman, W. T. & Adelson, E. H. The Design and Use of Steerable Filters. *IEEE Trans Pattern Anal Mach Intell* **19**, 801–906 (1991).
25. Jacob, M. & Unser, M. Design of steerable filters for feature detection using canny-like criteria. *IEEE Trans Pattern Anal Mach Intell* **26**, 1007–1019 (2004).
26. Carlsson, A., Håkansson, K., Kvick, M., Lundell, F. & Söderberg, L. D. Evaluation of steerable filter for detection of fibers in flowing suspensions. *Experiments in Fluids* **51**, 987–996 (2011).

Acknowledgements

Author contributions

A.M. and C.K. designed and performed all experiments, evaluated the data and wrote the manuscript. P.E.W. evaluated the data and handled all animal work. A.C. wrote the automated detection algorithm and evaluated the data. S.L.N., M.P.B. and J.M.C. wrote and edited the manuscript. M.P.B. and J.M.C. coordinated and supervised the work.

Additional information